Arbuscular mycorrhizal fungus Rhizophagus irregularis expresses an outwardly Shaker-like channel involved in potassium nutrition of rice (Oryza sativa L.)

Claire Corratgé-Faillie, Layla Chmaiss, Houssein Zhour, Jean-Pierre Lolivier, Pierre-Alexandre Audebert, Xuan Thai Bui, Maguette Seck, Kawiporn Chinachanta, Cécile Fizames, Daniel Wipf, et al.

Main Manuscript for

Arbuscular mycorrhizal fungus *Rhizophagus irregularis* expresses an outwardly Shaker-like channel involved in potassium nutrition of rice (*Oryza sativa* L.).

Claire Corratgé-Faillie[(1)], Layla Chmaiss[(1)], Houssein Zhour[(1)], Jean-Pierre Lolivier[(1)], Pierre-Alexandre Audebert[(1)], Xuan Thai Bui[(1)], Maguette Seck[(1)], Kawiporn Chinachanta[(2)], Cécile Fizames[(1)], Daniel Wipf[(3)], Hervé Sentenac[(1)], Anne-Aliénor Very[(1)], Pierre-Emmanuel Courty[(3)], Doan Trung Luu[(1)]

[1] IPSiM, Univ Montpellier, CNRS, INRAE, Institut Agro, Montpellier, France

[2] Faculty of Agriculture, Chiang Mai University, Chiang Mai, Thailand

[3] Agroécologie, Institut Agro Dijon, CNRS, Université de Bourgogne, INRAE, Université de Bourgogne Franche-Comté, Dijon, France.

* Doan Trung Luu.

Email: doan.luu@cnrs.fr

Author Contributions: DTL and PEC designed research; CCF, LC, HZ, JPL, PAA, XTB, MS, CF, KC and DTL performed research; CCF, LC, HZ, JPL, PAA, XTB, MS, CF, KC and DTL analyzed data; and CCF, HS, AAV, PEC and DTL wrote the paper. DW, HS, AAV, PEC and DTL performed writing review and editing.

Competing Interest Statement: The authors declare no competing interest.

Classification: BIOLOGICAL SCIENCES / Microbiology

Keywords: Symbiosis, plant-microorganism interactions, mycorrhizal nutrient uptake pathway, salt stress tolerance, voltage clamp.

This PDF file includes:

Main Text
Figures 1 to 8
Supplementary data

Abstract

Potassium (K^+) plays crucial roles in many physiological, molecular and cellular processes in plants. Direct uptake of this nutrient by root cells has been extensively investigated, however, indirect uptake of K^+ mediated by the interactions of the roots with fungi in the frame of a mutualistic symbiosis, also called mycorrhizal nutrient uptake pathway, is much less known. We identified an ion channel in the arbuscular mycorrhizal (AM) fungus *Rhizophagus irregularis*. This channel exhibits the canonical features of Shaker-like channel shared in other living kingdoms and is named RiSKC3. Transcriptionally expressed in hyphae and in arbuscules of colonized rice roots, RiSKC3 has been shown to be located

in the plasma membrane. Voltage-clamp functional characterization in *Xenopus* oocytes revealed that RiSKC3 is endowed with outwardly-rectifying voltage-gated activity with a high selectivity for K^+ over sodium ions. RiSKC3 may have a role in the AM K^+ pathway for rice nutrition in normal and salt stress conditions. The current working model proposes that K^+ ions taken up by peripheral hyphae of *R. irregularis* are secreted towards the host root into periarbuscular space by RiSKC3.

Significance Statement

Mutualistic symbiosis with arbuscular mycorrhizal (AM) fungi are beneficial for about 80% of land plants thanks to an exchange of nutrients. The AM pathway responsible for potassium (K^+) nutrition of the plant is not known. Here we uncovered a key step of this phenomenon, by functionally characterizing the first transport system in the AM fungus *Rhizophagus irregularis*, and we univocally demonstrated that RiSKC3 is an K^+ outwardly-rectifying voltage-gated Shaker-like channel.

Main Text

Introduction

Potassium (K^+), by constituting 2% to 10% of plant dry matter, is the most abundant cation in plant tissues; thus it is an essential macronutrient for plants (1, 2). It plays crucial roles in many physiological, molecular and cellular processes, which include respiration, photosynthesis, osmoregulation, anion neutralization, enzyme activation, membrane transport. K^+ homeostasis consequently impacts overall plant growth and development (1, 2). Availability of K^+ in soil for plant uptake is restricted by leaching losses, its fixation to minerals such as feldspars or micas, and its relatively low diffusion rate, forcing the soils to be amended with fertilizers for crop quality and yields (3, 4). Unfortunately, those fertilizers are expensive to produce.

To bypass K^+ availability in soil, plants can express high-affinity transport systems for a more efficient uptake, exudate organic acids by the root system for better mineral solubilization, and engage symbiotic associations with soil-living microbes (5, 6).

Roots of around 90% of land plants interact with mycelium of various fungi in the frame of a mutualistic symbiosis in which both individuals benefit from the association (7). Root symbiosis with fungi improves plant fitness and growth, especially by facilitating plant mineral nutrition. At the interface between the two symbiotic partners, the fungus receives fixed carbon from the plant and, in exchange, secretes mineral nutrients, which are taken up by root cells. The most extensively documented effects on plant nutrition concern the acquisition of P and N (both NH_4^+ and NO_3^-). The beneficial effects on plant K^+ nutrition are much less documented (5). Among these associations, two forms are mainly studied due to their agricultural and ecological importance, arbuscular mycorrhizae and ectomycorrhizae.

Ectomycorrizal (ECM) symbiosis concerns roots of woody plants of boreal and temperate forest ecosystems (8). Fungus colonizes intra-radical tissues by forming a specific structure called the Hartig net. This latter develops between cells of epidermis and cortex (8). Besides direct taken up of K^+ from the rhizosphere via root epidermis and root hairs, another indirect uptake pathway, called the mycorrhizal pathway, via the fungal hyphae developed within root cortex cell-walls for plant nutrition has been described. Importantly, fungal K^+ transport systems involved mycorrhizal pathway have been reported in ECM fungi. Among them, in the frame of the interaction between ECM fungus *Hebeloma cylindrosporum* and *Pinus pinaster, three* fungus-specific tandem-pore outwardly rectifying K^+ (TOK) channels where described and one of them (HcTOK2.2) participate in the release of K^+ towards colonized *P. pinaster* roots (9). Also, downregulation of the channel *HcSKC*, which belongs to the Shaker family based on sequence analysis, affects the fungal K^+ homeostasis, alters the expression of other fungal K^+ transport systems, and attenuates mycorrhizal K^+ pathway in *P. pinaster* (10).

Arbuscular mycorrhizal (AM) symbiosis involves fungi of Glomeromycotina and roots of more than 80% of land plants (8, 11). Specifically, AM fungi colonize the root cortex of host plants, developing hyphae and branched structures, named arbuscules, in the cells. This development is the result of a complex molecular dialogue between the fungus and the plant (11). AM symbiosis improves plant mineral nutrition and thereby plant growth. K^+ enrichment in shoot was found 28% higher in AM over than non-mycorrhized (NM) plants (12). In addition, AM fungi have a critical role in improving plant tolerance to environmental constrains such as drought and salinity (13). Thus, in a meta-analysis, AM symbiosis has been shown to increase by 42% K^+ enrichment in shoot, to decrease sodium (Na^+) translocation to shoot and consequently to increase the shoot K^+/Na^+ ratio, a marker of plant adaptation to toxic Na^+ concentrations, in salt-stress conditions (12). Since ionic (K^+ and Na^+) homeostasis is one of the major

molecular mechanism involved in plant tolerance to salinity (14, 15), AM symbiosis may alleviate salt stress by improving K^+ nutrition and by a protective effect, since acting as a first barrier for ion selection during ion uptake from the soil by peripheral hyphae and/or during ion translocation to the plant (16).

To elucidate the mechanism underlying mycorrhizal K^+ pathway, transcriptome analysis of K^+ transport systems from both AM partners is central. Indeed, in the AM fungus *Rhizophagus irregularis* four sequences from an EST library were identified as K^+ transport systems (17). One sequence belongs to the HAK/KUP/KT transporter family, whose members share homology with bacterial KUP (K^+ Uptake) and fungal HAK (high-affinity K^+) transporters (1). Three other sequences belong to the large family of tetrameric voltage-dependent K^+ channels (KV), often called Shaker-like channels (SKC). The assembly of four subunits (alpha-subunits) forms a functional channel with a permeation pathway for K^+ in the centre of the structure. A canonical Shaker alpha-subunit is composed of a hydrophobic core displaying six transmembrane segments with both N- and C-terminal tails located in the cytosol. The first four transmembrane segments (S1-S4) constitute the voltage-sensing module. The fourth transmembrane segment (S4), which is enriched in positively charged residues, constitutes the voltage sensor. The pore-forming module is composed of S5, pore loop (P), and S6. Between the fifth (S5) and sixth (S6) transmembrane segments, a pore loop (P) harbours the canonical K^+ selectivity filter “TxGYG” (Thr-X-Gly-Tyr-Gly) found in animal and plant Shaker channels. In plant Shaker channels; the C-terminal region downstream of S6 is cytosolic and successively comprises, from N- to C-term, a C-linker, a cyclic-nucleotide binding domain (CNBD), an ankyrin domain (absent in some alpha-subunits), and a KHA domain rich in hydrophobic and acidic residues (1).

Here we provide the description of the first fungal member of the *Shaker*-like channel family. This channel, named RiSKC3, is present in the genome of the model AM fungus *R. irregularis*. To investigate its role in plant K^+ nutrition mediated by mycorrhizal pathway, we have used rice (*Oryza sativa*) as a partner of *R. irregularis*. RiSKC3 sequence exhibits canonical features of Shaker channels and was found specifically expressed in *R. irregularis* hyphae and arbuscules. It was shown to be localized in plasma membrane by heterologous expression in yeast. To assess its role, RiSKC3 has been functionally characterized by heterologous expression and by two-electrode voltage-clamp experiments in oocytes, which revealed that this channel exhibits outwardly rectifying K^+-selective channel features. Taken altogether, these results suggest that a part of K^+ taken by AM mycelium exploring the soil is

secreted through RiSKC3 channels, providing root cells with an exogenous source of this ion. Here we uncover a key step of the mycorrhizal pathway that corresponds to the beneficial part for the plant engaged in the AM symbiosis.

Results

Beneficial effects of inoculation with *R. irregularis* on plant growth and K^+ nutrition.

To assess the effects of inoculation with *R. irregularis* on plant growth and K^+ nutrition in controlled conditions, we performed a series of experiments with the short-live cycle rice cultivar Kitaake. We also addressed the response of plant-AM fungus symbiosis to K^+ availability, by growing the plants in pots filled with sand to control the amount of nutrients provided, and by watering with Yoshida-modified-solution containing either 0.8 mM or 16-fold less K^+ (0.05 mM), corresponding to normal or low condition, respectively. The NM plants treated with low-K^+ solution showed a significant reduction of shoot dry weight (~14%), K^+ content (~73%), and K^+ quantity (~80%) when compared with plants supplied with normal K^+ (Fig. 1). At 9 week-post-inoculation (wpi), colonization of the roots by *R. irregularis* was monitored by staining with Trypan Blue, and revealed no significant difference between the normal and low-K^+ conditions, **i.e.** with a mycorrhization frequency of ~75%, an intensity of the mycorrhizal colonization of ~25% and arbuscule abundance of ~10%. In K^+-normal condition, NM and AM plants did not exhibit difference in dry weight, K^+ content, and K^+ quantity (Fig. 1). In contrast, in low-K^+ condition, AM plants exhibited an increase in dry weight, K^+ content and K^+ quantity, when compared with NM plants, by ~17%, ~48%, and ~58%, respectively (Fig. 1).

Beneficial effects of inoculation with *R. irregularis* on tolerance to salt stress.

Since K^+ homeostasis is crucial for plant tolerance to salinity, we addressed the beneficial effects of AM inoculation. A mild salt stress was applied for a week, following 8 wpi. Here again, for low-K^+ condition, AM plants exhibited higher dry weight, K^+ content and K^+ quantity than NM plants, by ~24%, ~52% and ~64%, respectively (Fig. 2). Plants subjected to salt stress undergo Na^+ translocation to the shoot. Low Na^+ content in shoot and consequently a high K^+/Na^+ ratio are recognized as indicators of plant tolerance to salinity. Here we observed that NM plants exhibited higher (~44%) Na^+ contents in shoots in low-K^+ than in normal condition (Fig. 2D). As a consequence, in conjunction with a lower K^+ content in the shoot due to low-K^+ condition, the K^+/Na^+ ratio was 5.7 fold lower in low-K^+ condition than in normal condition

(Fig. 2E). Importantly, in low-K^+ condition, AM inoculation of rice plants reduced Na^+ content of shoot tissues by ~20% (Fig. 2D). This and the increase in K^+ contents due to mycorrhization (Fig. 2C) resulted in a strong increase in K^+/Na^+ ratio, by 3-fold when compared with NM plants (Fig. 2E).

In silico analysis of the putative K^+ transport systems involved in the mycorrhizal K+-translocation pathway

Our previous data indicate that *R. irregularis* provides a mycorrhizal pathway that improves rice K^+ nutrition. To uncover the underlying mechanisms, *in silico* analyses were carried out to shed light on the putative K^+ transport systems involved. On the fungal side, *R. irregularis* only exhibits four candidate genes with EST sharing homology with K^+ transporters or channels characterized in plant, animal, bacteria and/or yeast (6, 18). Among these sequences, three share homologies with voltage-gated K^+ channels from the so-called Shaker superfamily (19-22). The corresponding genes were named RiSKC 1, 2 and 3, for *Rhizophagus irregularios* Shaker K^+ channel 1-3. Within this set of 3 K^+ transport proteins, RiSKC2 and RiSKC3 share the highest level of sequence homology (Fig. 3A). RiSKC1 clusters with fungal K^+ channel sequences from *H. cylindrosporum* and *Laccaria bicolor* (Fig. 3B). It is worth noting that none of these RiSKC channels clusters with canonical vShaker-like sequences from photosynthetic or animal organisms (Fig. 3B).

RiSKC3 exhibits the canonical features of Shaker family

We chose RiSKC3 for further investigation. Submitting RiSKC3 protein sequence to CD-search server, we identified a conserved Ion_trans domain (PF00520) corresponding to a transmembrane ion channel family, consisting of tetrameric Na^+, K^+, and Ca^{2+} ion channels, in which two C-terminal transmembrane helices flank a loop which determines ion selectivity of the channel pore (Fig. 4). Next, to refine its structure we submitted RiSKC3 protein sequence to a series of servers dedicated to the prediction of transmembrane helices (Fig.4). The hydrophobicity profile of the submitted sequence generated by the servers revealed the presence of 6-7 hydrophobic domains. The amino acid alignment of RiSKC3 with AtKAT1 from *Arabidopsis thaliana* or HsKv4.2 from *Homo sapiens* as templates for modelling confirmed the presence of 6 conserved transmembrane domains and one pore domain characterized by the GYGD motif ensuring K^+ selectivity (Fig. 4). The putative S4 segment (constituting the voltage sensor in Shaker channels) harbored 5 (~16%) positively charged arginine (R) or lysine (K) residues (R265, R271, R274, K280, R290) that have been shown in other Shaker channels to contribute to the channel voltage

sensitivity and gating charge (23). The putative cytosolic C-terminal consisting of 311 amino-acid residues did not exhibit the typical cyclic nucleotide-binding domain (CNBD), ankyrin and KHA domains present in several Shaker channels from plants.

RiSKC3 transcripts are localized in hyphae and arbuscules.

To assess the role of RiSKC3 in mycorrhizal pathway, the localization of its encoding transcripts was analysed in 9-wpi rice roots. Firstly, on the plant side, RT-PCR allowed the amplification of rice housekeeping gene *ubiquitin-like protein SMT3* in both NM and AM conditions (Fig. 5). Also, the *phosphate transporter OsPT11* (AF536960) which was identified as specifically expressed under AM condition (24) was detected only in AM condition (Fig. 5). On the fungal side, the housekeeping gene *cyclophilin-like domain-containing protein* was detected only in AM condition. Importantly, RT-PCR allowed the detection of *RiSKC3* transcripts only in AM condition and the relative quantification obtained by means of RT-qPCR revealed that the transcripts accumulated in the same manner in low-and normal external K^+ conditions (Fig. 5). The cellular localization of *RiSKC3* transcripts was analyzed by means of *in situ* RT-PCR experiments to take advantage of the high level of sensitivity of this technique in detecting low levels of transcripts. Endogenous phosphatase-alkaline activity was detected in fixed tissues (Fig. 6 A-B). However, when the tissues underwent the PCR cycles in the thermocycler, this endogenous activity vanished, allowing the detection of transcripts by means of phosphatase-alkaline activity (Fig. 6 C-D). Transcripts of *OsPT11* were detected in root cell colonized by an arbuscule, but not in hyphae (Fig. 6 E-F). Importantly, transcripts of *RiSKC3* were detected in arbuscules and hyphae (Fig. 6 G-H).

RiSKC3 is a plasma membrane-localized protein

To determine whether RiSKC3 functions as a plasma membrane protein, its subcellular localization was investigated by means of heterologous expression of its coding sequence fused in frame with the eGFP reporter gene and downstream of the *Saccharomyces cerevisiae phosphoglycerate kinase* (*PGK*) promoter in the pFL61 yeast expression vector. The construct was stably expressed in yeast. Samples were stained using FM4-64, a plasma membrane-specific dye. Confocal microscopy showed a colocalization of the GFP and FM4-64 fluorescence in the cells expressing the construct, providing evidence that RiSKC3 encode a plasma membrane-localized K^+ channel (Fig. 7).

Functional characterization in Xenopus oocytes.

To further investigate the functional properties of RiSKC3, electrophysiological analyses after heterologous expression in Xenopus oocytes were carried out. Using two electrode voltage-clamp technique, we observed that RiSCK3 expression resulted in an outwardly-rectifying current in oocytes injected with *RiSKC3* cRNA. Typical recordings obtained in control oocytes injected with water and in RiSKC3-expressing oocyte upon depolarization of the membrane in external medium containing 10 mM K^+ are shown in Figure 8A. The macroscopic current displayed great magnitude with slow activation and slow deactivation kinetics. Increasing the external K^+ concentration from 10 to 100 mM resulted in a small decrease in K^+ outward current as shown on I–V (current-voltage) curves (Figure 8B).

Selectivity of RiSKC3 was then investigated by replacing K^+ in the external medium by several alkali cations (Na^+, Li^+, Rb^+, Cs^+ or $NH4^+$) at the same 100 mM concentration. No significative modification of outward K^+ current was observed as shown by the I-V curves (Figure 8C). By determining the current reversal potential (Erev) from classical tail-current recording analyses, relative permeability ratios (to K^+) were calculated using the Goldman-Hodgkin-Katz equation, which revealed the following permeability order: $K^+ > Rb^+ >> NH_4^+ > Cs^+ > Na^+ > Li^+$ (Figure 8C bottom panel). The relative permeability of RiSCK3 to Rb^+ is high (0.82), whereas that to Na^+ is relatively weak.

Same tail-current analysis was then performed to determine the Erev shifts upon replacement of 100 mM K^+ in external medium by 10 mM K^+. This resulted in a -51 mV shift for a 10-fold decrease in external K^+ concentration. This shift (close to the predicted theoretical shift of -58 mV upon a 10-fold change in K^+ concentration for a channel that would be exclusively permeable to K^+) indicated that RiSKC3 displays a relatively high selectivity for K^+.

The experimental curves describing the voltage-dependency of the channel relative open probability (Po/Pomax) obtained from RiSKC3 deactivation currents (recorded at -20 mV after pre-pulses varying from -110 to +145 mV in the presence of 10 or 100 mM external K^+) were fitted with the classical two-state Boltzmann law as displayed in Figure 8E. The results indicate that the channel half-activation potential (Ea50, the membrane potential at which the channel relative open-probability is 0.5) is dependent on the external K^+ concentration, being shifted by -35 mV when this concentration was decreased from 100 to 10 mM (Figure 8E).

At last a series of experiments aimed at determining the pH sensitivity of RiSKC3 was performed. Comparison of the I–V curves obtained at pH 5.5, 6.5 and 7.5 in the presence of 100 mM K^+ in the

external medium revealed that RiSKC3 is activated by the acidification of the external medium, being increased by 170% at pH 5.5 (Figure 8F).

Discussion

Beneficial interactions between terrestrial plants and AM fungi correspond to the most ancient and widespread symbiosis in nature (25). This symbiosis is characterized by the exchange of nutrients between both partners. For its growth, development and reproduction, AM fungus is entirely dependent on photosynthetically fixed organic carbon and lipid supply by the plant (11). Reciprocally, water and mineral nutrients are translocated from the soil to the plant by the fungus (11, 26). Besides the beneficial effects of nutrient exchanges, AM symbiosis has been shown to improve plant tolerance to biotic and abiotic stresses (13, 27). For instance, a large number of studies concluded to the effects of AM symbiosis on enhancement of plant tolerance to salt stress, demonstrating the high interest for the use of biologically-based strategies for alleviating environmental constraints on plant production. It is likely that the molecular mechanisms underlying the beneficial effects of AM symbiosis rely on osmotic and ionic adjustment (14). Interestingly, a meta-analysis was conducted on 650 studies gathering 60 species and 46 genera in 17 families of host plants, and 21 AM fungal species in nine genera and six families. It was concluded that, among 22 solutes analysed after exposure to salt stress, AM symbiosis had very small effects on Ca^{2+} and Mg^{2+} concentrations but resulted in a significant K^+ enrichment and a higher K^+/Na^+ ratio in shoot and root (12). Moreover, the beneficial effects of AM symbiosis on plant parameters are variable according to the K^+ supply and plant species analysed (28, 29). This set of data points to the importance of understanding the plant nutrition of K^+ by the AM pathway.

In our study, addressing the plant beneficial effects in the model rice-*R. irregularis*, we came to the conclusion of an effect on K^+ nutrition: we observed a higher shoot dry mass and K^+ content in AM than in NM rice plants in low K^+ availability conditions. This result does not imply the absence of AM K^+ pathway in K^+ sufficient conditions (since AM colonization was observed similar in both K^+ conditions, data not shown). K^+ deficiency has been shown to provoke limited root development and reactive oxygen species accumulation in root tissues (30). Importantly, AM symbiosis not only improves plant K^+ nutrition, but also modulates the expression of specific root genes to cope with K^+ deficiency stress (28). Altogether, this set of data highlight the importance of AM pathway for plant nutrition for such an

essential nutrient. Unfortunately, knowledge on molecular players for such an important biological function in agroecosystem is still scarce.

On the plant side, the only K^+ transport systems so far identified were KT/KUP/HAK transporters that were shown to be up-regulated in AM roots of *Lotus japonicus* and *Solanum lycopersicum* compared to the NM roots (29, 31). In the case of tomato, *SlHAK10* was specifically expressed in the cells colonized by the arbuscules and could have a role in the mycorrhizal K^+ uptake pathway. In another plant model, although AM symbiosis improves the K^+ nutrition of *Medicago truncatula*, no K^+ transport systems was observed to be up-regulated in mycorrhizal roots (28). In rice, similar result on absence of up-regulated K^+ transport systems in AM- compared to NM-roots was found, suggesting that OsK1.1 (also named OsAKT1), OsHAK1, and OsHAK5, likely the three major K^+ transport systems natively expressed in roots, might play a role in AM K^+ pathway for plant nutrition (24, 32-34).

On the AM fungal side, although the transportome equipment has been described *in silico* for the fungal model *R. irregularis*, only few nutrient transport systems have been studied at transcriptomic level, and none has been functionally characterized so far (18, 35). Here we describe the first functional characterization of an AM fungal K^+ transporter. Among the sequences identified in *R. irregularis* as displaying homologies with K^+ transport systems from other kingdoms, *RiSKC3* sequence encoded a protein exhibiting the canonical features of Shaker-channel family with 6 putative conserved transmembrane domains, and one pore domain characterized by the GYGD motif ensuring K^+ selectivity. However, the putative S4 segment, shown to constitute the voltage sensor domain in voltage-gated K^+ channels, exhibits only 5 positively charged residues, a number lower than in other canonical channels (23). Also, RiSKC3 exhibits a putative cytosolic C-terminal region barely longer than the fungal HcSKC of *H. cylindrosporum* (10), but with none known domains. In animal kingdom, the C-terminal region mediates channel clustering by scaffold proteins (36). In plant kingdom, this cytosolic region includes several functional domains: (i) a linker region (C-linker) at a close distance to the pore that transduces conformational changes responsible for gating the channel, (ii) a CNBD mediating the interactions between subunits within the channel tetramer, (iii) an ankyrin domain mediating the binding of interacting proteins, and (iv) a KHA domain rich in acidic and hydrophobic residues, specific to plant K^+ channels, and involved in channel tetramerization and clustering at the membrane. The role of C-terminal region of RiSKC3 in clustering or intrinsic-activity regulation needs further investigation.

We univocally identified RiSKC3 functioning as a plasma membrane voltage-gated outwardly-rectifying K^+ channel. Importantly, RiSKC3 exhibited, in our conditions of analysis, a high selectivity for K^+ ions, suggesting its specific involvement in the AM K^+ pathway. Moreover, its higher intrinsic activity upon external acidic-pH conditions is consistent with its putative function in the secretion of K^+ in the periarbuscular space. Indeed, secreted K^+ ions might be bathed in an acidic environment to be further taken up by plant periarbuscular membrane transport systems. These latter systems might be endowed with H^+:K^+ symport activity, like HAK members shown to mediate active K+ uptake (Véry et al., 2014), and thus be activated by acidic conditioins.

This study performed in the rice model uncovered a key step in AM K^+ pathway and might be transposed to the whole interactions between other plant species and the AM fungus *R. irregularis*. Moreover, this discovery is of interest for biologically-based mechanisms involved in plant salt tolerance. The current working model proposes that uptake of K^+ ions from soil solution by an unidentified *R. irregularis* K^+ uptake transport system is followed by secretion into the periarbuscular space mediated by RiSKC3. The role of RiSKC3 in the secretion of K^+ ions is of fundamental importance since these ions might be afterwards absorbed by yet unidentified K^+ uptake transport systems tentatively located in the plant plasma-membrane facing the periarbuscular membrane. Identification of K^+ uptake systems in both *R. irregularis* and rice involved in the AM pathway deserves further investigation.

Materials and Methods

Plant Materials and Growth Conditions

Rice (*Oryza sativa* L.) ssp. Japonica cv. Kitaake plants and spores from *Rhizophagus irregularis* DAOM197198 (PremierTech, France) were used in this study. Seeds were germinated in a greenhouse for a week. Conditions of the greenhouse were 16 h of day cycle (~ 200 µE m^{-2} sec^{-1}) and 8 h of night at 28°C and 70% relative humidity. Next, for AM fungus inoculation, the seedlings were transplanted to sterilized quartz sand in a 6 cm × 6 cm × 7.5 cm planting pot and a suspension of ~500 spores of *R. irregularis* was added per pot containing one unique plant. For NM condition, inoculation with spores was omitted. Plants subjected to normal K^+-condition (0.8 mM K^+) were irrigated with Yoshida's modified-solution (37) containing the following: 0.5 mM $(NH_4)_2SO_4$, 1.6 mM $MgSO_4$, 1.2 mM $Ca(NO_3)_2$, 0.7 mM KNO_3, 60 µM $FeSO_4$, 60 µM Na_2EDTA, 20 µM $MnSO_4$, 0.32 µM $(NH_4)_6Mo_7O_{24}$, 1.4 µM $ZnSO_4$, 1.6 µM $CuSO_4$, 45.2 µM H_3BO_3 and 0.25 mM NaH_2PO_4, 0.1 mM K_2SO_4; solution was adjusted at pH 5-

5.5. Plants subjected to low K^+-condition (0.05 mM K^+) were irrigated with a solution containing the following: 0.5 mM $(NH_4)_2SO_4$, 1.6 mM $MgSO_4$, 1.2 mM $Ca(NO_3)_2$, 0.05 mM KNO_3, 60 µM $FeSO_4$, 60 µM Na_2EDTA, 20 µM $MnSO_4$, 0.32 µM $(NH_4)_6Mo_7O_{24}$, 1.4 µM $ZnSO_4$, 1.6 µM $CuSO_4$, 45.2 µM H_3BO_3 and 0.25 mM NaH_2PO_4, 0.65 mM $NaNO_3$; solution was adjusted at pH 5-5.5.

Salt treatment

Nine-week-old rice plants (corresponding to 8 wpi) were subjected to salt treatment by watering with 30 mL of a Yoshida solution supplemented with 100 mM NaCl. This provided to each pot 3 mmoles of Na^+. Next the plants were watered with a solution depleted of NaCl, but at a volume avoiding the leaching of Na^+ salt out of the pot, to maintain salt treatment. Control plants were watered with Yoshida solution depleted of NaCl during the whole of their life.

Quantification of K^+ and Na^+ contents

Shoots were collected and weighed to determine the dry biomass (DW). Ions were extracted from the tissues in 0.1 N HCl for 3 days and assayed by flame spectrophotometry (SpectrAA 220FS, Varian).

Phylogenetic tree construction

The protein sequences of SKC of *R. irregularis* (taxid:747089), *Hebeloma cylindrosporum* (taxid:76867), *Laccaria bicolor* (taxid:29883), *Physcomitrella patens* (taxid:3218), *Arabidopsis thaliana* (taxid:3702, *Drosophila melanogaster* (taxid:7227), *Homo sapiens* (taxid:9606), *Escherichia coli* (taxid:562) were collected from databases by BLASTP analysis based on RiSKC3 (Supplemental Table S1) and submitted to MUSCLE software for multiple alignment (38). The phylogenetic tree was generated with PhyML software (http://www.phylogeny.fr) using the maximum likelihood method (1000 bootstraps) and the tree was visualized by iTOL software (https://itol.embl.de/).

***In silico* analysis of RiSKC3 conserved protein domains**

CD-search server (https://www.ncbi.nlm.nih.gov/Structure/bwrpsb/bwrpsb.cgi) was used to identify conserved domains in RiSKC3 protein. Hydrophobicity profiles of RiSKC3 subunit was obtained using following servers: DAS-TMfilter (https://mendel.imp.ac.at/DAS/), HMMTOP (http://www.enzim.hu/hmmtop/index.php), MEMSAT-SVM analysis method of PSIPRED Workbench (http://bioinf.cs.ucl.ac.uk/psipred), SPLIT 4.0 (http://split.pmfst.hr/split/4/), SWISS-MODEL (https://swissmodel.expasy.org/) with AtKAT1 (7cal.1.A) or HsKv4.2 (7f0j.1.A) as a template for

modelling, Phobius (https://phobius.sbc.su.se/index.html), TMHMM (https://dtu.biolib.com/DeepTMHMM), TOPCONS (https://topcons.cbr.su.se/pred/).

RNA extraction and transcript analysis

Total RNAs were extracted from roots collected at same times using the RNeasy plus mini kit with gDNA eliminator according to manufacturer's instructions (Qiagen, Germany). First-strand cDNAs were synthesized from 3 µg of RNAs using SuperScript III reverse transcriptase (Invitrogen) according to manufacturer's instructions and used as template for RT-PCR or qRT-PCR experiments. PCR was performed as follows: 1 µL of cDNA (~50 ng), 10 µL of 5x Green GoTaq® Reaction Buffer (Promega), 1µL of dNTP Mix (10 mM each of dTTP, dCTP, dGTP, dATP), 5 µL of each of forward and reverse primers (10µM, Supplemental Table 2), 0.25 µL of GoTaq® DNA Polymerase (5 U/µL, Promega), and 27.75 µL of ultra-pure water. PCR cycles (95°C for 2 min, and 30 cycles at 95°C for 30 sec, 60°C for 30 sec, 72°C for 30 sec and 72°C for 5 min) were performed in a FlexCycler^2 (Analytikjena Biometra GmbH, Germany). The resulting PCR products were analysed by electrophoresis, stained with ClearSight DNA stain (Euromedex, France), and gel was scanned with Gel Doc^{TM} EZ Imager (Biorad). qRT-PCR analyses were performed using the Lightcycler480 system (Roche diagnostics) and SYBR *Premix Ex Taq* (Takara) in a total volume of 10 µL, which contained 2 µL of cDNA, 3 µL of forward and reverse primer mixture (1 µM, Supplemental Table 2), and 5 µL of SYBR *Premix Ex Taq*. Reactions were performed with three independent biological replicates, each one with three technical replicates (PCR program: 95°C for 30 sec; 45 cycles of 95°C for 10 sec, 60°C for 10 sec, and 72°C for 15 sec; followed by a melt cycle from 60°C to 95°C). C_T (cycle threshold) values were obtained from amplification data using a threshold of 0.37.

Liquid-phase *in situ* RT-PCR in rice roots

The present protocol is modified from (39). Roots were cut into 1 cm small pieces and immediately fixed in PAA [2% (v/v) paraformaldehyde, 63% (v/v) ethanol, 5% (v/v) acetic acid] overnight at 4°C. Fixed root pieces were washed three times for 10 min each in DEPC-treated water. For reverse transcription, sections were incubated at 65°C for 5 min in a tube containing the following: 2 µL of oligo(dT)$_{20}$ (50 µM); 2 µL of 10 mM dNTP Mix (10 mM each dATP, dGTP, dCTP and dTTP); 20 µL of ultra-pure water. Then the tubes were returned to ice before adding: 8 µL 5X First-Strand Buffer of SuperScript™ III RT kit (Invitrogen); 2 µL of 0.1 M DTT; 2 µL of RNaseOUT™ Recombinant RNase Inhibitor (40 units/µL,

Invitrogen); 2 µL of SuperScript™ III RT (200 units/µL, Invitrogen). The tubes were incubated at 42°C for 1 h. The sections were washed once with DEPC-treated water. For PCR reaction, the sections were added with: 10 µL of 5x Colorless GoTaq® Reaction Buffer (Promega); 1µL of dNTP Mix (10 mM each of dTTP, dCTP, dGTP, dATP); 0.5µL of digoxigenin-11-dUTP (1nmol/µL, La Roche, Meylan, France); 5 µL of each of forward and reverse primers (10µM, Supplemental Table S2), 0.25 µL of GoTaq® DNA Polymerase (5 U/µL, Promega), and 28.25 µL of ultra-pure water. PCR cycles (95°C for 2 min, and 30 cycles at 95°C for 30 sec, 60°C for 30 sec, 72°C for 30 sec and 72°C for 5 min) were performed in a FlexCycler^2 (Analytikjena Biometra GmbH, Germany). Following RT-PCR, the tubes were washed three times for 10 min in 1x PBS (5 mM Na_2HPO_4, 130 mM NaCl, pH 7.5). After blocking with 2% (w/v) BSA in 1x PBS for 1 h, sections were incubated with alkaline phosphatase-conjugated anti-digoxigenin-Fab fragment (La Roche) diluted 1:250 in blocking solution for 2 h. The sections were rinsed three times with 10x washing buffer (100 mM Tris–HCl, 150 mM NaCl, pH 9.5) for 15 min each. Detection of alkaline phosphatase was carried out for ~1 h using NBT/BCIP ready-to-use stock solution (La Roche) diluted in 1x washing buffer.

Plasmid construction for expression of RiSKC3-GFP construct

A pFL61 plasmid (Genbank X62909) harbouring the construct *HcTOK1-GFP* under the control of the *Saccharomyces cerevisiae phosphoglycerate kinase* (*PGK*) promoter was obtained from (10). PCR amplification allowed to remove the *HcTOK1* sequence, with reaction containing: 1 µL of pFL61[HcTOK1-GFP] (~100 ng), 10 µL of 5x Phusion® HF Buffer (Thermoscientific), 1µL of dNTP Mix (10 mM each of dTTP, dCTP, dGTP, dATP), 5 µL of each of *UAL* forward and *LAPGF* reverse primers (10µM, Supplemental Table S2), 0.5 µL of Phusion® DNA Polymerase (Thermoscientific), and 27.5 µL of ultra-pure water. PCR cycles (95°C for 2 min, and 25 cycles at 95°C for 30 sec, 60°C for 30 sec, 72°C for 3 min and 72°C for 5 min) were performed in a FlexCycler^2 (Analytikjena Biometra GmbH, Germany). *RiSKC3* cDNA fragment was amplified by PCR: 1 µL of pGEM[RiSKC3] (~100 ng), 10 µL of 5x Phusion® HF Buffer (Thermoscientific), 1 µL of dNTP Mix (10 mM each of dTTP, dCTP, dGTP, dATP), 5 µL of each of *UA846* forward and *LL846* reverse primers (10µM, Supplemental Table S2), 0.5 µL of Phusion® DNA Polymerase (2 U/µL, Thermoscientific), and 27.5 µL of ultra-pure water. PCR cycles (95°C for 2 min, and 25 cycles at 95°C for 30 sec, 60°C for 30 sec, 72°C for 1 min and 72°C for 5 min) were performed in a FlexCycler^2 (Analytikjena Biometra GmbH, Germany). The resulting PCR products were analysed by electrophoresis, stained with ClearSight DNA stain (Euromedex, France), and gel was

scanned with Gel Doc™ EZ Imager (Biorad). DNA fragments were excised from the gel by means of x-tracta™ Gel Extractor (Promega) and purified using Wizard® SV Gel and PCR Clean-Up System (Promega). Next, the In-Fusion HD Cloning Kit (Clontech, Mountain View, CA, USA) was used for cloning *RiSKC3* into pFL61 [GFP] plasmid: 2 µL of 5x In-Fusion HD Enzyme Premix (Clontech); 1 µL of linearized pFL61 [GFP] (~100 ng); 1 µL of *RiSKC3* fragment (~50ng); 6 µL of ultra-pure water. The tube was incubated for 15 min at 50°C, then placed on ice. Next 1 µL of In-Fusion reaction was used to transform Stellar™ competent cells (Clontech). DNA plasmids were sequenced using the service of Eurofins Genomics (Germany).

Heterologous expression in yeast

Saccharomyces cerevisiae strain PLY232 was used for heterologous expression of *RiSKC3-GFP* construct. Plasmid pFL61 harbouring the construct *RiSKC3-GFP* under the control of the *PGK* promoter was purified from Stellar™ bacteria using the PureYield™ Plasmid Miniprep System (Promega). The yeast transformation method was described by (40).

Confocal microscopy visualization

A laser scanning confocal microscope (Leica TSC SP8 system, Germany) was used with the excitation wavelengths 488 nm and 561 nm for GFP and FM4-64, respectively. The detection wavelengths were in the range of 500-535 nm for GFP and 580-630 nm for FM4-64.

Statistical Analysis

The data were analyzed by ANOVA, followed by Student's *t*-test to test differences between treatments.

Acknowledgments

This research was supported by the CultiVar project funded through ANR (the French National Research Agency) under the "Investissements d'avenir" programme with the reference ANR-10-LABX-001-01 Labex Agro and coordinated by Agropolis Fondation under the frame of I-SITE MUSE (ANR-16-IDEX-0006). This project was also supported by a Junior Research Fellowship Program from France Embassy in Thailand awarded to Dr Kawiporn Chinachanta. Confocal observations were performed at the Montpellier RIO Imaging facilities.

References

1. Nieves-Cordones M, Al Shiblawi FR, & Sentenac H (2016) Roles and Transport of Sodium and Potassium in Plants. *The Alkali Metal Ions: Their Role for Life*, eds Sigel A, Sigel H, & Sigel RKO (Springer International Publishing, Cham), pp 291-324.

2. Amrutha RN, Sekhar PN, Varshney RK, & Kishor PBK (2007) Genome-wide analysis and identification of genes related to potassium transporter families in rice (Oryza sativa L.). *Plant Sci* 172.
3. Rengel Z & Damon PM (2008) Crops and genotypes differ in efficiency of potassium uptake and use. *Physiol Plant* 133(4):624-636.
4. Zörb C, Senbayram M, & Peiter E (2014) Potassium in agriculture – Status and perspectives. *Journal of Plant Physiology* 171(9):656-669.
5. Haro R & Benito B (2019) The Role of Soil Fungi in K+ Plant Nutrition. *International Journal of Molecular Sciences* 20(13):3169.
6. Garcia K & Zimmermann SD (2014) The role of mycorrhizal associations in plant potassium nutrition. *Frontiers in Plant Science* 5(337).
7. Wang B & Qiu YL (2006) Phylogenetic distribution and evolution of mycorrhizas in land plants. *Mycorrhiza* 16(5):299-363.
8. Smith SE & Read DJ (2002) *Mycorrhizal Symbiosis* (Academic Press, London) p iv.
9. Guerrero-Galán C*, et al.* (2018) Plant potassium nutrition in ectomycorrhizal symbiosis: properties and roles of the three fungal TOK potassium channels in Hebeloma cylindrosporum. *Environmental Microbiology* 20(5):1873-1887.
10. Garcia K*, et al.* (2020) Fungal Shaker-like channels beyond cellular K+ homeostasis: A role in ectomycorrhizal symbiosis between Hebeloma cylindrosporum and Pinus pinaster. *PloS one* 15(11):e0242739-e0242739.
11. Lanfranco L, Fiorilli V, & Gutjahr C (2018) Partner communication and role of nutrients in the arbuscular mycorrhizal symbiosis. *New Phytol.* 220(4):1031-1046.
12. Augé RM, Toler HD, & Saxton AM (2014) Arbuscular mycorrhizal symbiosis and osmotic adjustment in response to NaCl stress: a meta-analysis. *Frontiers in Plant Science* 5(562).
13. Begum N*, et al.* (2019) Role of Arbuscular Mycorrhizal Fungi in Plant Growth Regulation: Implications in Abiotic Stress Tolerance. *Frontiers in Plant Science* 10(1068).
14. Munns R & Tester M (2008) Mechanisms of Salinity Tolerance. *Annual Review of Plant Biology* 59(1):651-681.
15. Shabala S & Cuin TA (2008) Potassium transport and plant salt tolerance. *Physiologia Plantarum* 133(4):651-669.
16. Porcel R, Aroca R, Azcon R, & Ruiz-Lozano JM (2016) Regulation of cation transporter genes by the arbuscular mycorrhizal symbiosis in rice plants subjected to salinity suggests improved salt tolerance due to reduced Na+ root-to-shoot distribution. *Mycorrhiza* 26(7):673-684.
17. Gutjahr C*, et al.* (2015) Transcriptome diversity among rice root types during asymbiosis and interaction with arbuscular mycorrhizal fungi. *Proceedings of the National Academy of Sciences* 112(21):6754-6759.
18. Casieri L*, et al.* (2013) Biotrophic transportome in mutualistic plant–fungal interactions. *Mycorrhiza* 23(8):597-625.
19. Yellen G (2002) The voltage-gated potassium channels and their relatives. *Nature* 419(6902):35-42.
20. Jan LY & Jan YN (2012) Voltage-gated potassium channels and the diversity of electrical signalling. *The Journal of physiology* 590(11):2591-2599.
21. Véry A-A*, et al.* (2014) Molecular biology of K+ transport across the plant cell membrane: What do we learn from comparison between plant species? *Journal of Plant Physiology* 171(9):748-769.
22. Jegla T, Busey G, & Assmann SM (2018) Evolution and Structural Characteristics of Plant Voltage-Gated K+ Channels. *The Plant Cell* 30(12):2898-2909.
23. Seoh S-A, Sigg D, Papazian DM, & Bezanilla F (1996) Voltage-Sensing Residues in the S2 and S4 Segments of the Shaker K+ Channel. *Neuron* 16(6):1159-1167.
24. Güimil S*, et al.* (2005) Comparative transcriptomics of rice reveals an ancient pattern of response to microbial colonization. *Proceedings of the National Academy of Sciences* 102(22):8066-8070.

25. Parniske M (2008) Arbuscular mycorrhiza: the mother of plant root endosymbioses. *Nature Reviews Microbiology* 6(10):763-775.
26. Quiroga G*, et al.* (2019) The arbuscular mycorrhizal symbiosis regulates aquaporins activity and improves root cell water permeability in maize plants subjected to water stress. *Plant Cell Environ* 42(7):2274-2290.
27. Campo S*, et al.* (2020) Effect of Root Colonization by Arbuscular Mycorrhizal Fungi on Growth, Productivity and Blast Resistance in Rice. *Rice* 13(1):42.
28. Garcia K, Chasman D, Roy S, & Ané J-M (2017) Physiological Responses and Gene Co-Expression Network of Mycorrhizal Roots under K^+ Deprivation. *Plant Physiology* 173(3):1811-1823.
29. Liu J*, et al.* (2019) The Potassium Transporter SlHAK10 Is Involved in Mycorrhizal Potassium Uptake. *Plant Physiology* 180(1):465-479.
30. Shin R & Schachtman DP (2004) Hydrogen peroxide mediates plant root cell response to nutrient deprivation. *PNAS* 101.
31. Guether M*, et al.* (2009) Genome-wide reprogramming of regulatory networks, transport, cell wall and membrane biogenesis during arbuscular mycorrhizal symbiosis in Lotus japonicus. *New Phytol.* 182(1):200-212.
32. Chen G*, et al.* (2015) Rice potassium transporter OsHAK1 is essential for maintaining potassium-mediated growth and functions in salt tolerance over low and high potassium concentration ranges. *Plant, Cell & Environment* 38(12):2747-2765.
33. Yang T*, et al.* (2014) The Role of a Potassium Transporter OsHAK5 in Potassium Acquisition and Transport from Roots to Shoots in Rice at Low Potassium Supply Levels. *Plant Physiology* 166(2):945-959.
34. Li J*, et al.* (2014) The Os-AKT1 Channel Is Critical for K+ Uptake in Rice Roots and Is Modulated by the Rice CBL1-CIPK23 Complex. *The Plant Cell* 26(8):3387-3402.
35. Garcia K, Doidy J, Zimmermann SD, Wipf D, & Courty P-E (2016) Take a Trip Through the Plant and Fungal Transportome of Mycorrhiza. *Trends in Plant Science* 21(11):937-950.
36. Magidovich E, Orr I, Fass D, Abdu U, & Yifrach O (2007) Intrinsic disorder in the C-terminal domain of the Shaker voltage-activated K+ channel modulates its interaction with scaffold proteins. *Proceedings of the National Academy of Sciences of the United States of America* 104(32):13022-13027.
37. Yoshida S, Forno DA, Cook JH, & Gomez KA (1976) *Laboratory manual for physiological studies of rice* (International Rice Research Institute, Manila).
38. Edgar RC (2004) MUSCLE: multiple sequence alignment with high accuracy and high throughput. *Nucleic Acids Research* 32(5):1792-1797.
39. Cellier F*, et al.* (2004) Characterization of AtCHX17, a member of the cation/H+ exchangers, CHX family, from Arabidopsis thaliana suggests a role in K+ homeostasis. *The Plant Journal* 39(6):834-846.
40. Gietz RD & Schiestl RH (1991) Applications of high efficiency lithium acetate transformation of intact yeast cells using single-stranded nucleic acids as carrier. *Yeast* 7.

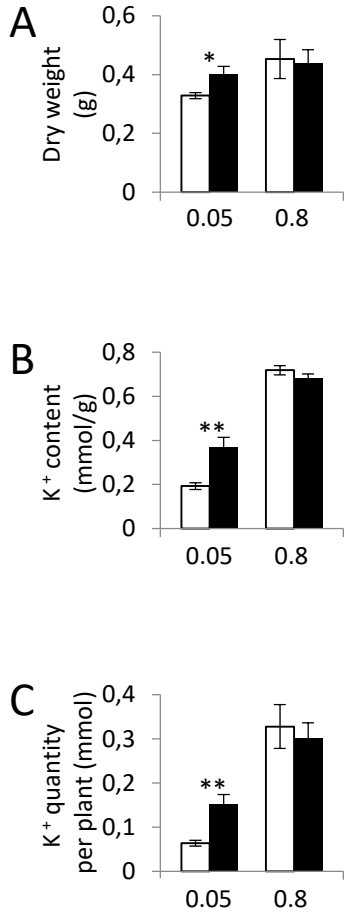

Figure 1. Effects of *R. irregularis* inoculation on *O. sativa* growth and K^+ nutrition.
Rice plantlets were germinated on water for a week, then not- (opened bars) or inoculated (closed bars) with ~500 spores of *R. irregularis.* Plants were watered with a nutrient solution containing either 0,05 mM or 0,8 mM K^+, for 9 weeks, before tissue harvesting. Dry weight (g, **A**), K^+ content (mmol/g DW, **B**), K^+ quantity per plant (mmol, C) in shoot are represented. Watering condition with nutrient solution containing either 0,05 or 0,8 mM K^+ are represented on left and right, respectively. The mean values and SEMs are indicated from two independent series of experiments, with a total number of plants of ten. Significant differences between not- and inoculated conditions, based on Student's *t*-test, are shown (** $P<0,001$, * $P<0,05$).

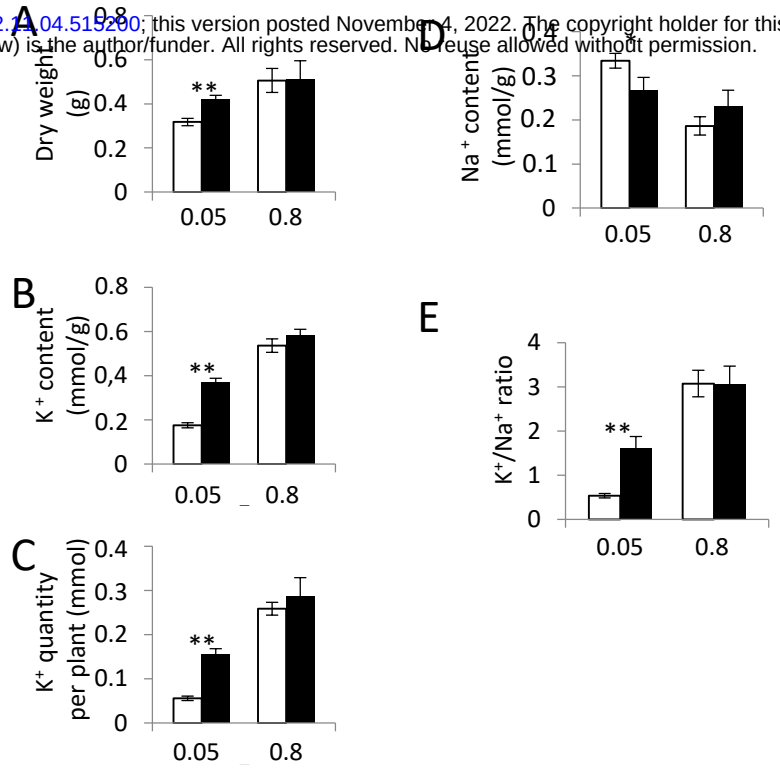

Figure 2. Effects of *R. irregularis* inoculation on *O. sativa* growth, K^+ nutrition and Na^+ uptake under salt stress.

Rice plantlets were germinated on water for a week, then not- (opened bars) or inoculated (closed bars) with ~500 spores of *R. irregularis.* Plants were watered with a nutrient solution containing either 0.05 mM or 0.8 mM K^+, for 8 weeks. Afterwards, plants subjected to salt stress received a nutrient solution supplemented with 100 mM NaCl (the total quantity of Na^+ per pot was 3 mmoles) and continued to be watered without Na^+ for a week, before tissue harvesting. Dry weight (g, **A**), K^+ content (mmol/g DW, **B**), K^+ quantity per plant (mmol, **C**), Na^+ content (mmol/g DW, D), K^+/Na^+ ratio (E) in shoot are represented. Watering condition with nutrient solution containing either 0.05 or 0.8 mM K^+ are represented on left and right, respectively. The mean values and SEMs are indicated from two independent series of experiments, with a total number of plants of ten. Significant differences between not- and inoculated conditions, based on Student's *t*-test, are shown (** *P*<0,001, * *P*<0,05).

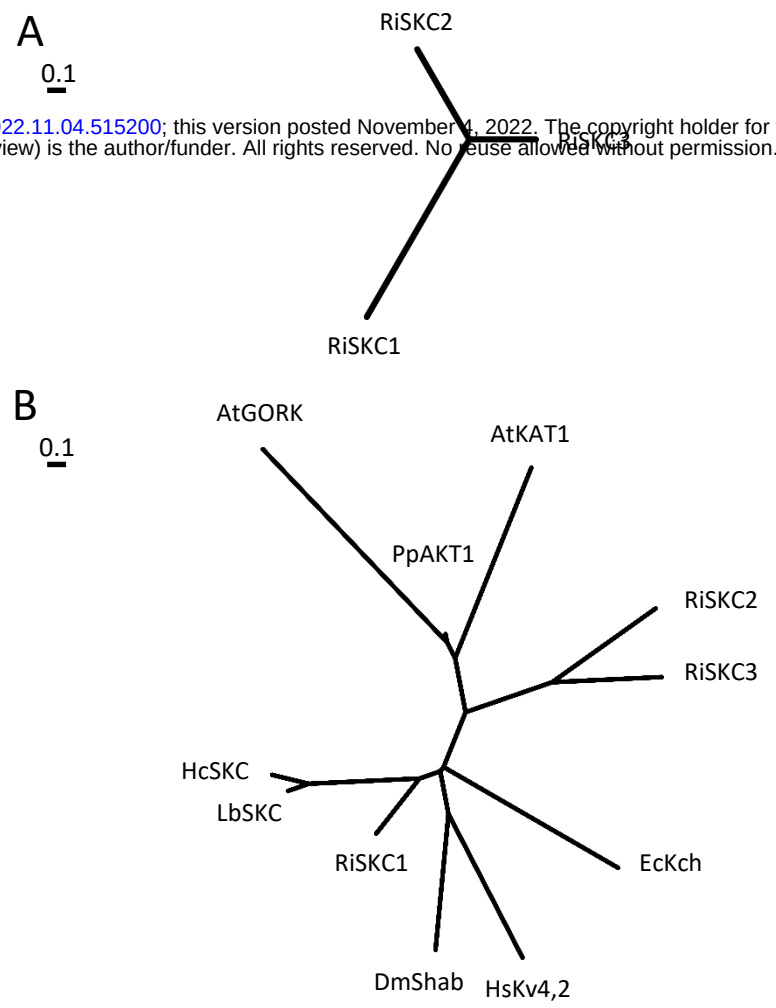

Figure 3. Phylogenetic analysis of Shaker channels in *R. irregularis*.
The phylogenetic tree was generated with PhyML software (http://www.phylogeny.fr) using the maximum likelihood method. The branch length is proportional to the number of substitutions per site. The bar provides a scale of number of substitutions per site. The protein (GenBank) accession numbers are given in Supplemental Table S1. **A.** *R. irregularis* Shaker-like K^+ channels (RiSKC) sequences in *R. irregularis* were compared to each other. **B.** RiSKC3 sequence was compared to the following sequences from *R. irregularis*, *Hebeloma cylindrosporum* (taxid:76867, HcSKC), *Laccaria bicolor* (taxid:29883, LbSKC), *Physcomitrella patens* (taxid:3218, PpAKT1), *Arabidopsis thaliana* (taxid:3702, AtKAT1, AtGORK), *Drosophila melanogaster* (taxid:7227, DmShab), *Homo sapiens* (taxid:9606, HsKv4,2), *Escherichia coli* (taxid:562, EcKch).

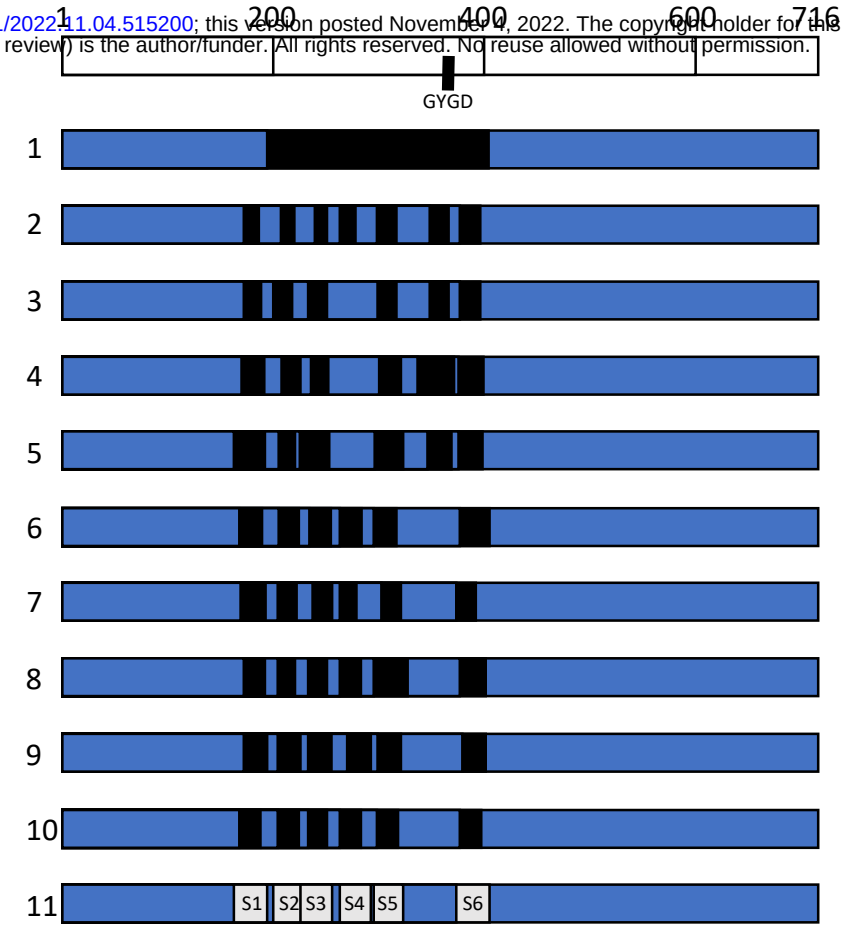

Figure 4. Secondary structure analysis of RiSKC3.

RiSKC3 protein sequence is represented as a bar with residue positions indicated on the top. The position of conserved GYGD motif is indicated. CD-search server identified a conserved ion_trans domain (PF00520) represented in black (1). Positions of predicted transmembrane helices are represented as black bars after using DAS-TMfilter server (2), HMMTOP server (3), MEMSAT-SVM analysis method of PSIPRED Workbench (4), SPLIT 4.0 server (5), SWISS-MODEL server with AtKAT1 (7cal.1.A) or HsKv4.2 (7f0j.1.A) as a template for modelling, respectively (6 and 7), Phobius server (8), TMHMM server (9), TOPCONS server (10). Regions of the protein sequence where the six transmembrane helices (S1-S6) likely stand, according to the combination of the bioinformatics analysis are represented as white bars (11).

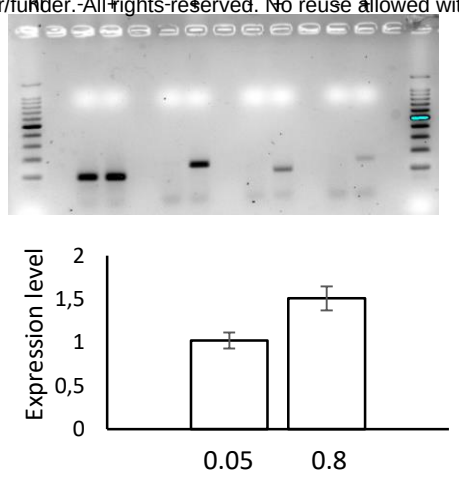

Figure 5. Expression level of *RiSKC3* in AM rice roots.

A-week-old plantlets of rice was not inoculated (-) or inoculated (+) with ~500 spores of *R. irregularis*. Plants were watered with a nutrient solution containing either 0.05 mM or 0.8 mM K^+, for 9 weeks. Next, roots were harvested and total RNA was extracted. (Upper) RT-PCR was performed to amplify ~100 bp fragments corresponding to *OsSMT3*, *OsPT11*, *RiCYP1*, and *RiSKC3* identified by an asterisk (Promega 100 bp DNA ladder was loaded at each border of the gel). (Lower) RT-qPCR was performed with ARN extracted from inoculated plants watered with nutrient solution containing either 0.05 or 0.8 mM K^+. The mean and SEMs of relative quantitative values are shown from a duplicate.

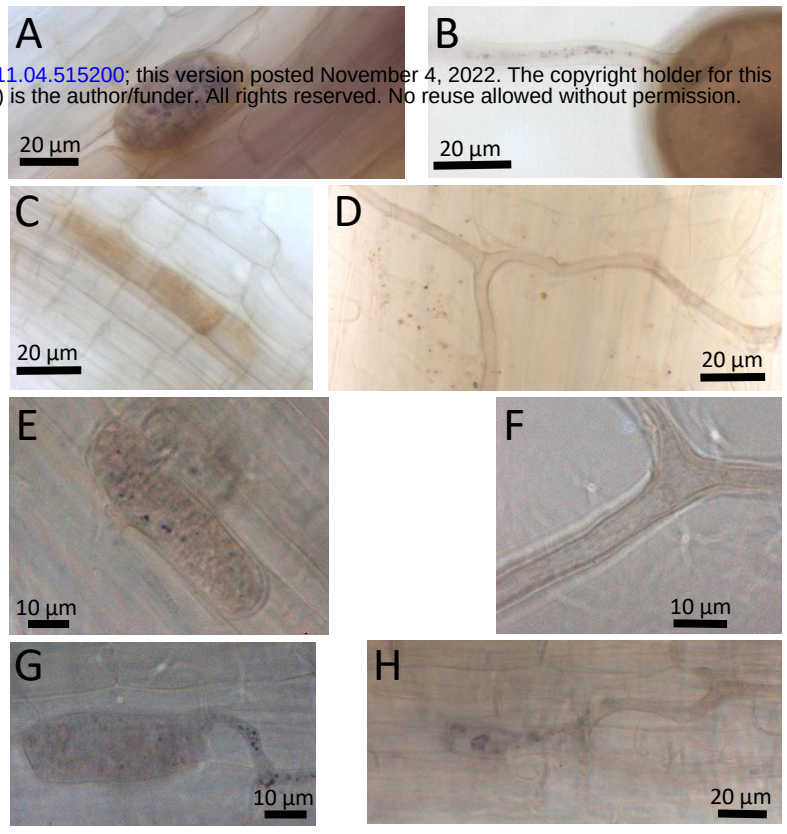

Figure 6. Expression pattern of RiSKC3 in AM rice roots.

Nine-week *R. irregularis* inoculated roots were subjected to whole-mount *in situ* RT-PCR. Fixed tissues were incubated with NBT/BCIP to detect endogenous phosphatase-alkaline activity in vesicles (**A**) and in hyphae emerging from a spore (**B**) as a purple precipitate signal. When fixed tissues were subjected to PCR cycles without any reagent for labeling, and incubated with NBT/BCIP, endogenous phosphatase-alkaline activity was not detected in cells colonized by arbuscule (**C**) nor in extraradical hyphae (**D**). *In situ* RT-PCR was performed with primers specific to *OsPT11*; a signal was detected in a root cell colonized by an arbuscule (**E**), but not in extraradical hyphae (**F**). *In situ* RT-PCR with primers specific to *RiSKC3* allowed the detection of a signal in root cell colonized by an arbuscule (**G**) and in intraradical hyphae (**F**).

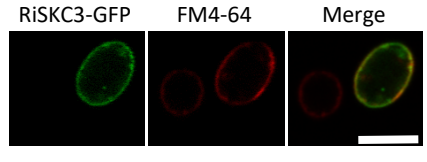

Figure 7. Subcellular localization of RiSKC3.

Yeast cell expressing RiSKC3-GFP construct was observed with confocal microscopy after staining with membrane-dye FM4-64, under GPA channel (left), FM4-64 channel (middle), allowing to reconstitute a merged image (right).

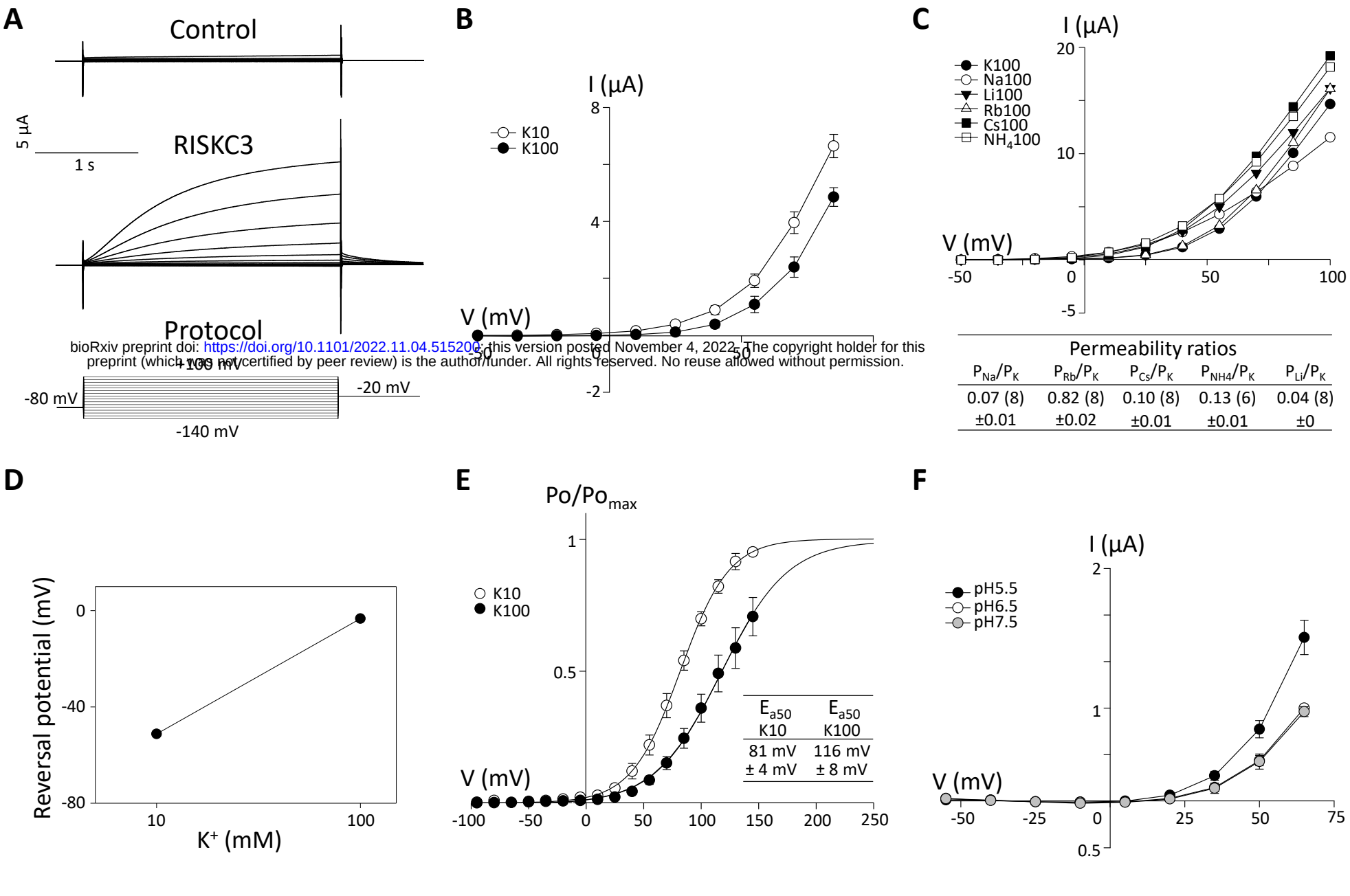

Figure 8. Functional characterization of RiSKC3 in *Xenopus* oocytes.

A. Typical currents recorded in control oocytes (injected with water) or in oocytes injected with *RiSKC3* cRNA in 10 mM KCl using a voltage clamp protocol (bottom panel) with voltage clamp pulses ranging from −140 to + 100 mV, in increments of 15 mV from a holding potential of -80 mV. **B.** RiSKC3 current–voltage relationships in 10 mM (white circles) or 100 mM KCl (black circles). Mean value ± SE, from n=4 oocytes. **C.** Permeability of RiSKC3 to different monovalent cations. Representative current–voltage relationships recorded in 100 mM of either K^+, Na^+, Li^+ Rb^+, Cs^+ or $NH4^+$. Permeability ratios of the different cations with respect to that of K^+, calculated from the variations of E_{rev} (obtained from tail currents) using the Goldman–Hodgkin–Katz equation. Ratios are given as mean ± SE (number of determination). **D.** Variation of RiSKC3 reversal potential (E_{rev}) in 10 mM and 100 mM KCl. E_{rev} was determined using a tail-current protocol: after activation of RiSKC3 at +55 mV, voltage pulses were performed at voltages flanking E_{rev}. **E.** Effect of the membrane voltage and the external K^+ concentration on RiSKC3 open probability. The relative open probability (Po/Po_{max}) was obtained from the analysis of deactivation currents upon return to the holding potential (mean ± SE, n=5). The solid lines are Boltzmann fits to the mean Po/Po_{max} values. The mean values (± SE, n=5) of the half-activation potential (E_{a50}) of RiSKC3 obtained from these fits in 10 mM or 100 mM of KCl are provided in the inset. **F.** Activation of RiSCK3 currents by external acidification. The external solution contained 100 mM KCl at pH 5.5, 6.5 or 7.5. Means ± SE, n = 4.

Supplemental Table S1. GenBank accession numbers of Shaker polypeptides present in phylogenetic trees

Gene name	Accession number	Protein ID
RiSKC1	GLOIN_2v1553770	XP_025183612.1
RiSKC2	GLOIN_2v1590016	XP_025179892.1
RiSKC3	GLOIN_2v1661846	XP_025172766.1
HcSKC		KIM34880
LbSKC		XP_001881176
PpAKT1		AM695749
AtKAT1		At5g46240
AtGORK		Q94A76
DmShab		P17970
HsKv4.2		XP_011514467.1
EcKch		WP_171459460.1

Supplemental Table S2. Primers used for PCR

Gene (experiment)	Primer name	Sequence (5'-3')	Amplicon length (bp)
OsSMT3 (qPCR)	QRT94SMT3-F	CCTCAAGGTCAAGGGACAGG	94
	QRT94SMT3-R	ACGGTCACAATAGGCGTTCA	
OsPT11 (qPCR & In situ)	OSPT11-F	CGCATGATACGCTCATCTGG	151
	OSPT11-R	CCAAGCTAGCATCTGGCAATT	
RiCYP1 (qPCR)	RICYP1-F	TTAAGACTCCCTGGCTAGATGGC	110
	RICYP1-R	GGAAGTTTTTCCACTGGATGAACCC	
RiSKC3 (qPCR & in situ)	RISKC3-F	TTCAATGTTGCAAAATACACAGTTGGC	143
	RiSKC3-R	CCACGTTCTATAAAATACATTATAGCTGAAGATGC	
pFL61 (RiSKC3-GFP)	UAL	TCGAGGGTGCCTGATCA	6173
	LAPGF	GCGGCCGCTGGTTTTATATTTGTTG	
RiSKC3 (RiSKC3-GFP)	UA846	AAAACCAGCGGCCGCATGTCTGAAAATAATGAAAAAGAA	2151
	LL846	ATCAGGCACCCTCGAAAAATTTTCATTATTCGAATTATTC	